

Research Article

Assiya Sarinova*, Leila Rzayeva, Alexandr Neftissov, Serimbetov Bulat, Lalita Kirichenko, Yerassyl Omirtay, Ansar Sansyrbayev, and Nursultan Kabenov

Comparison of Deep Learning-based Models for Detection of Diseased Trees using an Image Compression Algorithm

DOI: DOI, Received ..; revised ..; accepted ..

Abstract: This paper describes the application of machine learning to classify aerospace tree images obtained from a variety of sources, including satellites, drones, and aircraft. One of the urgent tasks is the archiving of images due to their large amount of disk space. Therefore, the study is aimed at the analysis and development of software that allows to compress images in order to reduce the volume they occupy, using new mathematical and adaptive compression algorithms to identify diseases in the phytosanitary control of forestry. Particular attention is paid to deep learning methods, such as convolutional and capsular neural networks, which have shown high efficiency and accuracy in image recognition and classification tasks. This paper presents a comparative analysis of the results of the work of three models based using YOLO v5, YOLO v7, and YOLO v8. The result of the suggested models' processing in the form on stage detection and classification of targeted images has maintained a high speed of learning and target objects detection, thereby increasing the correctness of detection. The best model YOLOv8 achieved high precision – 88.2%, recall 77.4%, mAP50 score 87.2% and average detection speed of single imagery is 0.052 s, and the model size is 21.5 MB. Overall, using machine learning for dead tree classification shows promise in combating global forest reduction and safeguarding ecosystems.

Keywords: Aerospace images, YOLO (You Only Look Once) model, Region Convolutional Neural Network (RCNN), Computer vision, Forest management.

1 Introduction

In the modern world ecology has a significant role in the sustainability of the planet. Over the past few decades, the world has witnessed a significant reduction in forest cover. According to alarming statistics,

***Corresponding Author: Assiya Sarinova:** Associated Professor of Astana IT University, 010000 Astana, Kazakhstan e-mail: assiya_prog@mail.ru

Leila Rzayeva: Assistant Professor of Astana IT University, 010000 Astana, Kazakhstan, e-mail: leilarza2@gmail.com

Alexandr Neftissov: Associated Professor of Astana IT University, 010000 Astana, Kazakhstan, e-mail: shurik-neftisov@mail.ru

Serimbetov Bulat: Associate Professor of the Department of Information Technology, Kazakh University of Technology and Business, 010000 Astana, Kazakhstan, e-mail: sba_rnmc@mail.ru

Lalita Kirichenko: Senior Lector of Astana IT University, 010000 Astana, Kazakhstan e-mail: sanzhar.kusdavletov@astanait.edu.kz

Yerassyl Omirtay: Junior Researcher of Astana IT University, 010000 Astana, Kazakhstan, e-mail: ilyaskazambayev@gmail.com

Ansar Sansyrbayev: Junior Researcher of Astana IT University, 010000 Astana, Kazakhstan, e-mail: lalita17021996@gmail.com

Nursultan Kabenov: Bachelor student of Astana IT University, 010000 Astana, Kazakhstan, e-mail: era-syl120902@gmail.com

: Bachelor student of Astana IT University, 010000 Astana, Kazakhstan, e-mail: ansariks@mail.ru

: Bachelor student of Astana IT University, 010000 Astana, Kazakhstan, e-mail: nursultankabenovv@gmail.com

deforestation has led to the loss of millions of hectares of forest area annually. Forest fires, rampant illegal logging, urban expansion, and the spread of diseases are among the key factors contributing to the decline in forested regions across the globe. Deforestation, driven by agricultural expansion, infrastructure development, and logging activities, continues to pose a severe threat to forest ecosystems. Additionally, diseases and pests have become more pervasive due to changing environmental conditions, affecting the health of trees and diminishing forest resilience. Therefore, the forest state monitoring for correct decision-making in forest management is relevant. Research and development of new technologies for precise monitoring and detection of the occurrence of diseases is an extremely important task in forestry management. For organization tree diseases monitoring there are several areas of survey methods have been studied, including X-ray and ultrasound technologies. Collecting data to obtain indicators for assessing the state of forests using a field survey is a rather complex process, expensive, time-consuming, and not exhaustive in spatial terms. However, it is difficult to assess and observe the diseased trees only based on field surveys. Alternatively, remote sensing provides a fast and cost-effective approach to obtaining such data. At the present stage, remote sensing technologies make it possible to cover large areas with sufficiently high accuracy in determining the state of forests. The problem of increasing huge volume of aerospace data replenishment of remote sensing of the Earth, which is transmitted via communication channels for further processing, classification and identification an actual research problem. Popular solutions in this field have average compression coefficients, low speed encoding, average quality of restoring aerospace data and high computational algorithms complexity. Frequently, modern methods are not enough to solve the problem, since the communication channel resources are limited and the quality requirements for transmitted data does not correspond, and the presentation of information is not possible in full measure. The analysis of well-known solutions of compression algorithms, such as the lossless data compression standard CCSDS (USA), spatial algorithms, common wavelet transformations, JPEG compression algorithm, specialized adaptive compression methods for specific aerospace images showed the existing disadvantages in compression speed, low coefficient and high computational complexity. Lossy compression methods demonstrate a low level of quality of the recovered images necessary for classification and identification for various tasks in agriculture, water industry and military-intelligence. In response to the urgent need for effective forest monitoring and disease detection, researchers and technologies are turning to innovative solutions that leverage advances in remote sensing and data processing technologies. A promising possibility is the integration of artificial intelligence (AI) and machine learning algorithms into remote sensing systems to analyze large amounts of aerial data more accurately and efficiently. Using the power of artificial intelligence, these systems can independently identify patterns, anomalies and potential indicators of tree disease with an accuracy and speed that cannot be achieved by manual methods. By learning from large data sets, machine learning algorithms can recognize subtle changes in forest conditions and detect early signs of disease or stress. This approach not only increases the overall efficiency of monitoring, but also enables proactive and timely interventions in forest management.

2 Related work

In the field of Earth remote sensing research, numerous approaches, methods, and algorithms have been developed for the processing, compression, encoding, and decoding of aerospace images. Compression methods can be broadly classified into two categories: lossless information and lossy decoded images.

Recent research [1] in the field of image compression has focused on addressing challenges, exploring opportunities, and identifying future research directions. In [2] the article proposed algorithm for lossless compression of images utilizes K-means clustering and parallel prediction, offering an adaptive prediction compression algorithm based on an absolute ratio for compressing two-dimensional nested images. This approach overcomes the limitations of traditional prediction algorithms, which operate in sequential processing mode and have long processing times. Another notable development [3] is the CCSDS-MHC algorithm, proposed by the advisory committee on the Space data system for lossless image compression.

This algorithm has been implemented in the Raspberry Pi 3 Model B+ system using open multiprocessing (OpenMP).

Many of the compression methods and algorithms discussed in the literature [8–15] are based on a single Aviris remote sensing data source, raising questions about their applicability to images from other satellites. These methods often rely on well-known and specialized solutions, such as preprocessing JPEG compression, the CCSDS standard, and SPIHT. However, these algorithms may not meet the requirements for quality, speed, computational complexity, and may not take into account the specific characteristics of aerospace images.

Lossy compression methods have been widely studied in the context of classification [16, 22, 23], recognition [18], clustering [17], and object identification in aerospace images [19–21]. Analysis of existing lossy compression methods for aerospace images has shown that they are commonly used in processing tasks [24–33].

The integration of deep learning and aerospace imagery for object detection represents a promising solution to address the pressing environmental concerns associated with declining forest health worldwide. As forests play a crucial role in maintaining ecological balance, monitoring their condition is of paramount importance. Traditional methods of tree inspection can be time-consuming and costly, but advancements in artificial intelligence (AI) and remote sensing technologies have opened up new avenues for efficient and accurate monitoring. The reviewed articles in the field of computer vision and deep learning demonstrate the transformative impact of these technologies.

In recent times, the discipline of computer vision has undergone remarkable expansion, characterized by a multitude of noteworthy discoveries and pioneering methodologies. This comprehensive assessment endeavors to accentuate a selection of particularly noteworthy scholarly papers that have imparted substantial advancements to this domain. These scholarly works exemplify the forefront of computer vision research, providing invaluable perspectives into the contemporary progressions and patterns within this swiftly burgeoning field.

In the article [34], a comprehensive approach is presented for detecting and classifying dead nematode-infested pine wood. This is achieved using sophisticated models such as You Only Look Once version 4 (YOLO v4) and Google Inception version 1 Net (GoogLeNet), which process high-resolution aerial images captured by helicopters. The outcomes are promising, with detection accuracy reaching 95% and classification accuracy at 85%.

Similarly, another article [35] contributes by examining various remotely sensed data sources for identifying standing dead trees. The proposed tree-based approach exhibits considerable potential in predicting the presence of standing dead trees across expansive landscapes.

In disaster management applications, a series of articles [36–38, 42] present effective methods for assessing the impact of disasters, detecting roads and airports, and identifying bamboo forests. This underscores the efficacy of deep learning techniques in disaster response scenarios.

Furthermore, object detection and counting in satellite imagery are significantly improved through remote sensing and image analysis techniques, as demonstrated in articles [39–41]. These studies elucidate the potential of deep learning in enhancing accuracy and efficiency within this context.

Contributions to image classification are also noteworthy. Several articles [43, 44, 48] systematically compare traditional machine learning algorithms with deep learning counterparts, elucidating the advantages of the latter. Authors [46, 47] introduce classification methods for satellite and aerospace images, employing Convolutional Neural Networks (CNNs) and mean shift procedures, respectively.

Moreover, deep learning methodologies have been harnessed in a variety of domains, such as remote sensing image retrieval, satellite image classification, and X-ray baggage security imagery [45, 49–55, 57]. These studies collectively underscore the potential of deep learning in enhancing the accuracy and efficiency of image analysis in these intricate applications.

Articles [56, 58] delve into a deep learning-based approach for identifying pine wilt trees, utilizing Unmanned Aerial Vehicles (UAVs) to gather data. Results consistently exhibit accuracies exceeding 91%, with the additional advantage of rapid detection speeds, as evidenced by an average processing time of 0.067 seconds per image in [59].

To conclude, the amalgamation of deep learning techniques and remote sensing has revolutionized computer vision. While these contributions are notable, the review underscores the necessity for a more coherent structure that comprehensively addresses global challenges in the field.

3 Methodology

Despite all noteworthy contributions from related works reviewed, there is a need for a more structured approach that addresses global challenges in a comprehensive manner of classification model development. In this paper we propose an algorithm for detecting diseased trees using the YOLO model with new preprocessing methodology of image compression. Fast inference speed images in real time of YOLO has proven to be a powerful tool for object detection, achieving impressive accuracy and real-time performance.

Our approach leverages the strengths of YOLO to accurately detect infected trees in aerial and satellite imagery. By combining deep learning with remote sensing data, our algorithm is able to distinguish between diseased and healthy trees with high accuracy. This has the potential to greatly improve our ability to monitor forest health and manage natural resources. Figure 1 explains the steps of creating a model based on YOLO.

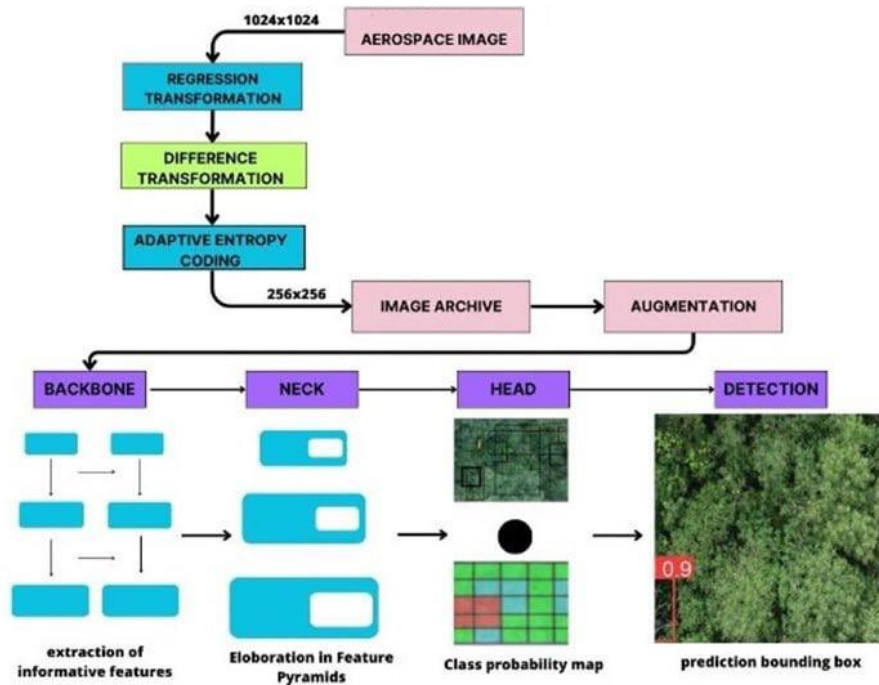


Figure 1. The structure of the training process

As can be seen in the Figure 1, the entire study is divided into two main stages: the description of a new algorithm for compressing images without loss of quality and the application of the results obtained for the classification model.

3.1 New image compression algorithm

The present research introduce developed and adapted for the classification of diseased trees and compression of images the mathematical apparatus based on the difference-discrete transformation. The sequence of stages of the proposed mathematical model is as follows:

1. Calculation of the correlation value between all pairs of image channels and determination of the channel encoding and decoding sequence;
2. Regression transformation algorithm;
3. Obtaining channel differences and their block-by-block conversion;
4. Compression by statistical algorithm.

Description of the lossless compression algorithm:

- *Step 1.* Let's calculate the values of the correlation matrix between all pairs of channels A and B, while identifying the most correlated groups of channel pairs. Based on the matrix, we will form and determine the sequence of transformation (encoding) and reverse transformation by constructing a strongly branching tree.
- *Step 2.* Regression analysis based on step 1. We calculate the linear regression coefficients between the values of the generative (the main vertex of the tree, BI) and the regressed (RI) channels of aerospace images by creating optimal values for the formation of arrays of differences between BI and RI.
- *Step 3.* Block-by-block conversion. The idea of the transformation is to calculate the differences based on step 2 by the block-by-block separation of data. The effectiveness of this separation is that the differences obtained do not cover the entire range of the image, but only a certain block. Due to this, they are effectively compressed by an entropy algorithm.
- *Step 4.* Compression by a well-known statistical algorithm.

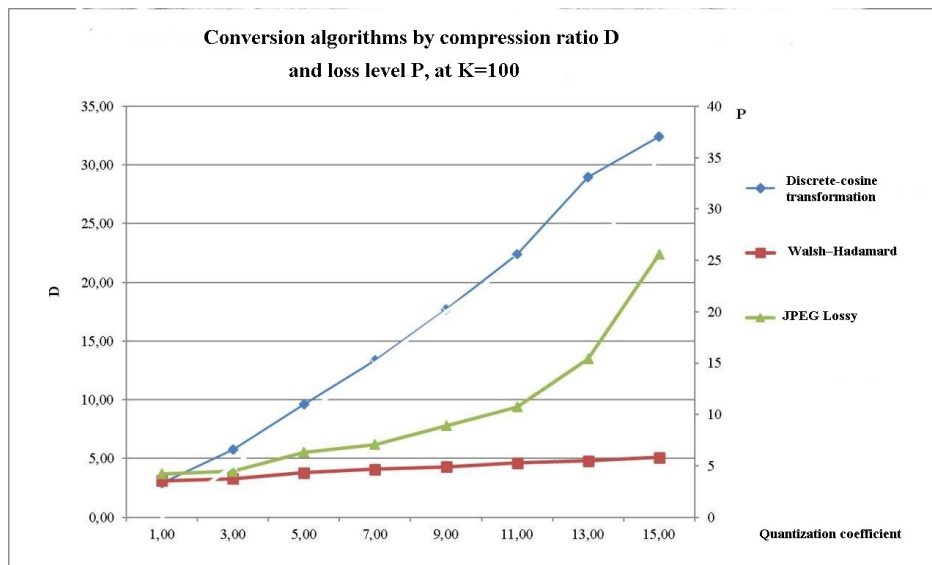


Figure 2. Conversion algorithms

Let's consider the proposed algorithm in detail.

Knowing that aerospace images are obtained in the spectrum of a single wave, we assume that some degree of dependence can be determined between pairs of channels. To determine the magnitude of this dependence, we use the Pearson correlation coefficient calculation formula (aka linear correlation coefficient). The formula requires two sequences of data, so we first extract two sequences of samples from a pair of files. This happens as follows: we represent a two-dimensional data matrix of one channel in the form of a linear

array (passing the matrix line by line from left to right and rows from top to bottom), then we select a certain number of samples in it (denote the number by the letter m ; dividing the array into approximately identical segments). From the second channel, we extract a sequence of samples that are located in the matrix at the same positions as the samples from the first channel. We denote the resulting sequences with the letters x and y , and the individual values are x_i and y_i (i from 1 to m inclusive). Also, the arithmetic averages of both sample sequences (1) will be needed for the formula.

$$\bar{x} = \frac{1}{m} \sum_{i=1}^m x_i, \bar{y} = \frac{1}{m} \sum_{i=1}^m y_i \quad (1)$$

Next, you need to apply the formula:

$$r = \frac{\sum_{i=1}^m (x_i - \bar{x})(y_i - \bar{y})}{\sqrt{\sum_{i=1}^m (x_i - \bar{x})^2 \sum_{i=1}^m (y_i - \bar{y})^2}} \quad (2)$$

Why we extract samples – for large channel matrices, calculating the formula for all values would take a huge amount of time. By setting the upper threshold for the number of samples, we remove the dependence of the calculation time on the image size.

By calculating the coefficients for all possible pairs of channels of the same image, we build a coding sequence – naturally, starting from large values to smaller ones.

Regression (regressive) transformation

The essence of the transformation is to bring into compliance with the encoded pair of channels some structure that would:

1. allowed to unambiguously restore one of the original channels according to the data of another channel,
2. occupied as little disk space as possible.

To do this, the following algorithm was defined. In each encoded pair of channels, we define a generating channel (master) and a regressed channel (slave, compressible). It has been experimentally confirmed that the principle of definition has a rather insignificant effect on the compression index; therefore, without wasting time on sorting through both options, we choose the channel with a smaller index as the generating channel (assuming that all channels were originally numbered).

Now let's explain how the difference matrix is considered (then it will be clear why the desired structure is so named). Before that, we calculated the linear correlation coefficient. The idea of linear regression in our case is to find such real values of k and b such that the matrix formed from the data of the encoded pair according to the following formula (3):

$$d_{ij} = (x_{ij} \times k + b) - y_{ij} \quad (3)$$

(here and further x_{ij} and y_{ij} – the values in the master and slave matrices, respectively) would have as small values as possible. Next, we will call the matrix d with the values d_{ij} «the difference matrix». A sufficiently good linear correlation indicator (close to one), calculated beforehand, leads to sufficiently low values d_{ij} . Knowing the values of k , b and the matrix d , can reconstruct the matrix y from the values of the matrix x (4):

$$y_{ij} = (x_{ij} \times k + b) - d_{ij} \quad (4)$$

Standard formulas used to calculate linear regression parameters (5):

$$k = \frac{\bar{x}\bar{y} - \bar{x} \times \bar{y}}{\bar{x}^2 - (\bar{x})^2}, b = \frac{\bar{x}^2 \times \bar{y} - \bar{x} \times \bar{x}\bar{y}}{\bar{x}^2 - (\bar{x})^2} \quad (5)$$

when \bar{x} will be calculated (6) and $\bar{x}\bar{y}$ (7):

$$\bar{x} = \frac{1}{i \times j} \sum_{i=1}^m \sum_{j=1}^n x_{ij}; \bar{y} = \frac{1}{i \times j} \sum_{i=1}^m \sum_{j=1}^n y_{ij} \quad (6)$$

$$\bar{x}\bar{y} = \frac{1}{i \times j} \sum_{i=1}^m \sum_{j=1}^n (x_{ij} \times y_{ij}); \quad \bar{x}^2 = \frac{1}{i \times j} \sum_{i=1}^m \sum_{j=1}^n x_{ij}^2 \quad (7)$$

(m – image height, n – width).

In each compressed channel, we put the values k and b in Double format (8 bytes, 15 decimal places in decimal format). By encoding the only main generating channel for the image (the generating channel of the first pair) independently of the others, will be able to restore it later in the first place, then gradually restore all the other compressed channels (as mentioned earlier, through the coefficients k and b).

The absence of losses is ensured during transformations. After receiving the matrix d and before writing it to the file, we round the values to the nearest integer (in the case of a fractional part equal to 0.5 – to a smaller integer). This does not prevent a lossless recovery. Let's explain why. Let's pay attention to the formula (3):

The matrices x and y are integers, so the value $w_{ij} = (x_{ij} \times k + b)$ has the same fractional part (let's denote it q) as the number d_{ij} before rounding. We will denote the integer part of the numbers through square brackets, the fractional part through curly ones. So, $q = \{d_{ij}\} = \{w_{ij}\}$

To reverse decode AI, we perform the following actions:

- *Step 1.* Decoding arrays of differences by the Huffman algorithm.
- *Step 2.* Formation of regression transformation arrays by finding the sums between the generating channel and its average value.
- *Step 3.* Formation of the initial arrays based on the available OHR coefficients and obtaining the initial data of AI.

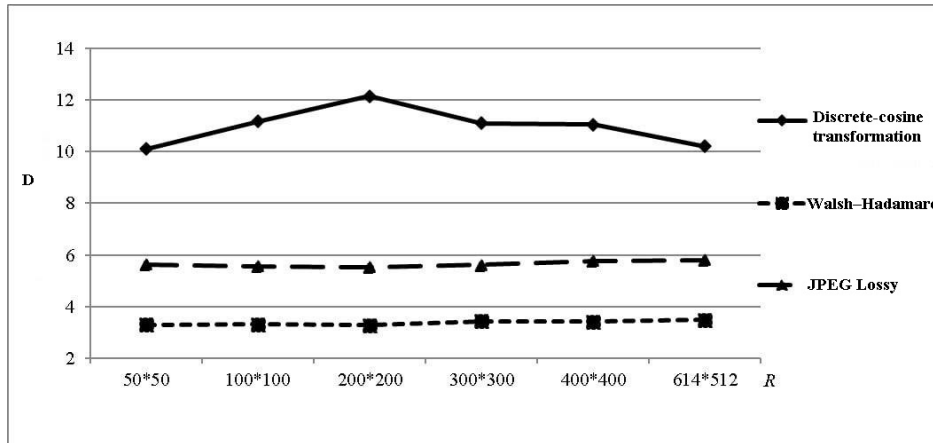



Figure 3. Comparison of three different processing methods

As a result, compression methods and algorithms were selected to develop methods of diseased tree control. Based on the above results of the compression experiment based on orthogonal and wavelet transformations of aerospace images with losses, it can be concluded that the developed mathematical and software compression, to some extent occupies a leading position in the degree of compression and quality of the restored images, depending on the selected preparatory processing, significantly demonstrates and surpasses analogues on all test sets.

Based on the conducted research, the following conclusions are made:

- The development of algorithms based on discrete-difference transformations allows to increase the compression ratio to $R = 12$.
- The proposed lossy approach is determined in adaptive transformations based on the Walsh-Hadamard transformation, discrete-cosine transformation and the generated quantization table and subsequent adaptive coding.

Table 1. Recognition classification model dataset after augmentation stage

Category	Example Image	Number of Training Set Samples	Number of Testing Set Samples	Number of Validation Set Samples
Diseased tree		724	63	63

- The obtained results of comparing the transformed AI using the obtained coefficients suggest the effectiveness of using these studies with adaptive Huffman coding.
- A comparison of quality criteria using standard quality metrics allows us to note that AI has been restored with high quality and minimal losses.

The results of experimental studies of the original algorithms are obtained in comparison with standard and specialized analogues in terms of compression ratio, computational and efficiency presented [59]. It is noted that lossless compression algorithms, taking into account inter-band correlation, using difference-discrete transformations, are superior to other algorithms in terms of a set of indicators.

3.2 Design of Deep Learning-based Models for Detection of Diseased Trees

Acknowledged best architecture solution YOLO have been chosen for creating deep learning classification models based on above explained image resize approach. For optimizing NN training process the images dataset has been converted from dimension 1024x1024 to 256x256 by coding the proposed mathematical algorithm. The aerospace images after the regression transformation, difference transformation and adaptive entropy coding stages were saved to image archive with compression ratio of $R=8$. This scientific approach substantiates the project's methodical preparation for forthcoming developmental stages.

From image archive already compressed without losses images dataset underwent augmentation leveraging the aforementioned platform, a process that engendered an enhanced volumetric representation while concurrently refining its inherent quality. The expanded corpus is now poised for the subsequent phase of model refinement, encompassing the conversion of dataset information into the YOLO format, a task seamlessly executed within the same digital ecosystem.

The initial series of JPEG images, designed for the purpose of developing target detection models was divided in an 8:1:1 ratio. As a result, 150, 20, and 22 images were respectively assigned to the training, validation, and test subsets. To develop a high-quality classification model, it is necessary to prepare a data set with a large number of images. To enrich the training set, augmentation procedures such as image flipping, scaling, and color dithering were employed. Notably, the augmentation process was deliberately withheld from the validation and test sets to ensure the reliability of unbiased estimates. The application of this augmentation methodology expand dataset to obtain a total of 850 images. The Table 1 describe divided for training, testing and validation steps data.

The dataset comprises a collection of visual data depicting forested environments featuring the presence of trees exhibiting pathological conditions. Each image in the dataset has been meticulously labeled and annotated, rendering it suitable for utilization in the training of deep learning models aimed at automated disease detection and classification within arboreal populations.

Various image augmentation techniques were employed to enhance the dataset. These techniques encompassed transformations such as rotation, grayscale conversion, shear, blur, and the addition of noise. A visual representation of a subset of these augmentation methods is depicted in Figure 4.

The subsequent phase marks the commencement of the model training process, a pivotal stage in the project's progression. To facilitate this essential task, the decision has been made to leverage Google Colab, a highly regarded cloud-based platform renowned for its provisioning of the Jupyter notebook environment,

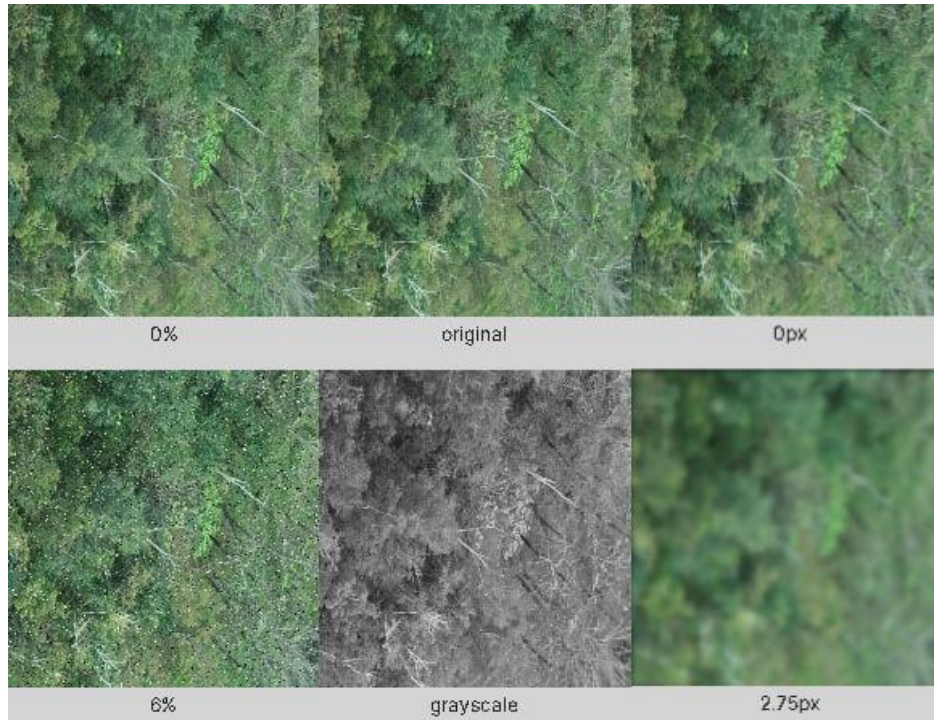


Figure 4. Image Augmentation process

coupled with robust computational resources. This choice is underpinned by Colab's widespread adoption within the machine learning community, attributed to its unparalleled accessibility and formidable computational capabilities.

Within the ambit of this training endeavor, the spotlight is cast upon three distinguished models: YOLOv5, YOLOv7, and YOLOv8. These models, known for their advancements in object detection and localization, have been thoughtfully selected for training and subsequent comparison. By adopting this meticulous comparative analysis, we aim to discern the model that exhibits the highest performance characteristics, effectively encapsulating accuracy, efficiency, and robustness.

Upon the conclusion of the training phase, an intricate evaluation will be conducted, delving into the nuances of each model's capabilities, strengths, and weaknesses. This comprehensive assessment will serve as the linchpin for identifying the model that surmounts its counterparts, emerging as the optimal choice for the current project's objectives.

The models underwent training using conventional configurations, forming the foundation for the experimental phase. Within the framework of expanding these models, specific modifications were introduced to enhance the learning process. It is of significance to highlight the deliberate reduction of input photograph resolution to 256x256 pixels. This reduction was implemented with the intent of augmenting the model's perceptual efficiency.

To ensure the preservation of image fidelity amidst the compression process, a lossless algorithm for compressing aerospace images was adopted. This algorithm, as elucidated earlier, employs regression techniques.

Furthermore, the number of epochs, a crucial parameter influencing the depth of training, was subject to adjustment. In the case of the YOLOv7 model, a configuration was established wherein 54 epochs were executed. In contrast, the remaining models underwent training over the course of 100 epochs. This divergence in epoch count could signify varying degrees of convergence and refinement, warranting thorough investigation and analysis.

A discernible divergence in learning rates was also evident among these models. To provide a succinct overview, the learning rates were tailored differently across the spectrum of models. A more detailed

breakdown of these learning rate differentials can be observed in the accompanying table 2. Such a strategic manipulation of learning rates can potentially influence the pace and efficacy of learning, underscoring the nuanced approach undertaken in the training of these expanded models.

	YOLOv5	YOLOv7	YOLOv8
Training time	3600 s	8020.8 s	7596 s
Average training time per round	35 s	134 s	70 s
Batch size	8	16	8
Epochs	100	54	100

Table 2. Experimental results of comparing different models implementation

In comparing YOLOv5, YOLOv7, and YOLOv8 based on training parameters:

- YOLOv5 exhibits the shortest training time and lowest average time per round.
- YOLOv7 shows extended training times and higher time per round due to its larger batch size.
- YOLOv8 offers competitive training times with a moderate batch size.

Considerations depend on project priorities: YOLOv5 for fast convergence, YOLOv7 for parallelism, and YOLOv8 for a balanced approach. Model performance assessment remains crucial for informed selection. The evolution of the models from their standard configurations involved a multifaceted strategy that encompassed resolution reduction, batch size augmentation, epoch count adjustment, and learning rate variation. These adaptations were orchestrated with the intention of cultivating a deeper understanding of how alterations in these parameters could impact the models' learning dynamics and eventual performance.

3.3 Result and discussions

The proposed lossless image compression approach is defined in adaptive transformations based on the Walsh-Hadamard transformation, discrete-cosine transformation and the generated quantization table and subsequent adaptive coding. In the course of the scientific research, the results of comparing the transformed aerospace images using calculated coefficients were obtained. The output test results suggest the effectiveness of using these studies with adaptive Huffman coding. The knowledge gained in the course of research allows us to determine the optimal parameters for compression:

1. The results of the compression ratio indicators improve with an increase in the size of the channels of parameter R . This is due to the fact that the more values to be converted, the fewer bits are required to store them;
2. The best values of the compression ratio are achieved by choosing the number of channels in an ordered group, with the limitations of the parameter $10 < K < 15$;
3. Taking into account the interchannel correlation of the Cor parameter shows that the greatest values in the compression ratio of the channel number, with variation of the parameter in the range $0 < N < 210$;
4. The algorithm, taking into account correlation and grouping at $G \in [2..10]$, shows the most effective growth in the compression ratio due to the formed groups of channels and their ordering.

The conducted studies of software compression without loss of quality of images for phytosanitary examination of trees in aerospace photography proves superiority over analogues and high performance. Therefore, this approach was applied to create a classification model for the recognition of infected trees based on YOLO.

The integration of deep learning in environmental monitoring provides valuable insights into forest conservation efforts. The ability to efficiently detect dead trees can help identify areas affected by deforestation, forest fires, and disease. Timely intervention in such areas can prevent further degradation and contribute to the conservation of forest ecosystems. By providing a reliable tool to identify diseased trees, proposed models will support ecosystem conservation efforts. Forest management authorities and environ-

mental agencies can integrate this technology to prioritize areas for restoration, implement sustainable practices, and effectively allocate resources. The outcome of diseased tree detection has view presented in Figure 5.

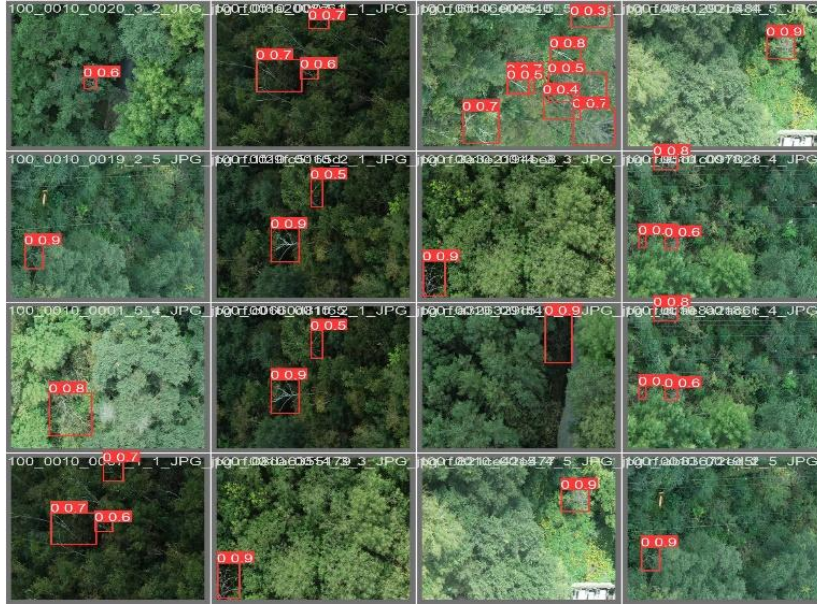


Figure 5. Displaying the recognized Diseased Trees on the image using the proposed model

The assessment of model performance was conducted through a meticulous analysis of a designated test set comprising various images. This test set served as a standardized benchmark against which the models' capabilities were rigorously evaluated. The utilization of a dedicated test set is a widely accepted practice in the realm of deep learning, enabling an objective measurement of the models' proficiency in real-world scenarios.

To render the evaluation process more insightful and visually informative, graphical representations were generated using the matplotlib library. These graphical outputs, meticulously crafted and thoughtfully designed, provided an illustrative depiction of the models' performance trends. By visualizing the data in this manner, intricate patterns, fluctuations, and comparative insights were readily discernible, facilitating a comprehensive understanding of how each model fared under differing circumstances.

The criteria of the obtained models developed on the basis of the YOLO architecture, well-known evaluation indicators be used, such as the average precision (mAP), the number of parameters (in MB) and the mean detection time (in seconds per sheet).

$$mAP = \frac{1}{N} \sum_{i=1}^N AP_i \quad (8)$$

The calculation of AP based on integral computation of the PR curve with Precision as the horizontal axis and Recall as the vertical axis. The precision indicator (P) affects classification ability to samples from a dataset, Recall R reflects the ability to find the positive sample and N represents the number of categories of data. The mAP parameter corresponding the average AP of all categories.

The Precision, Recall and F1 score was employed the following formulas:

$$R = \frac{TP}{TP + FN} \quad (9)$$

$$P = \frac{TP}{TP + FP} \quad (10)$$

In turn, the parameters P and R are calculated based on the values from the confusion matrix: TP (true positive), FP (false positive) and FN (False Negative). The number of positive samples with correct and incorrect model outcome accordingly described the TP (true positive) and FP (false positive) parameters. FN (false negative) indicates the number of negative samples with incorrect prediction. The metric F1 score present the harmonic mean precision and recall:

$$F1 = 2 \frac{P \times R}{P + R} \quad (11)$$

Positive and negative samples are evaluated by threshold the Intersection over Union (IoU) between the predicted and actual image's regions. In condition if both IoU parameters exceeding a certain threshold, then it is a positive sample, in other case it is a negative sample. Also for comparing of outcoms models results were calculated the average detection speed, which indicate average time the model spends to detect a single image in the validation set. All metrics results presented in Table 3.

	YOLOv5	YOLOv7	YOLOv8
Precision	99.7%	83.2%	88.2%
Recall	69%	71.2%	77.4%
mAP50	87.3%	85.2%	87.2%
F1-score	81%	77%	82%
Trained model size (in MB)	13.6	71.3	21.5
Detection time (in s/sheet)	0.079	0.123	0.052

Table 3. Experimental metrics results of different models

In this comparison of YOLOv5, YOLOv7, and YOLOv8 object detection models, several performance metrics were evaluated. YOLOv5 stands out with the highest precision (99.7%) but a relatively lower recall (69%), resulting in a balanced F1-score (81%). YOLOv7 offers a competitive precision (83.2%) and recall (71.2%), along with an mAP50 of 85.2% and an F1-score of 77%. YOLOv8 strikes a balance with precision (88.2%) and recall (77.4%), yielding an mAP50 of 87.2% and an F1-score of 82%. YOLOv5 has the fastest detection time (0.079s/img), YOLOv7 has a moderate detection time (0.123s/img), and YOLOv8 is the most efficient (0.052s/img). Selection among these models depends on specific task requirements, with YOLOv5 favored for accuracy and speed, YOLOv7 for well-rounded performance, and YOLOv8 for a balance between precision, recall, and speed.

All model classifying results in validation stage presented in figures 6-6.

The application of deep learning techniques to classify diseased trees from aerial imagery has important implications for environmental monitoring and forest management. This study examines the use of the You Only Look Once (YOLO) model and its performance in accurately detecting and classifying diseased trees. The results, challenges, and potential future developments in this area are also discussed.

The outcomes of the evaluation were notably impressive, with each model exhibiting distinctive results reflective of its unique characteristics and training nuances. The discernible variation in results across models underscores the significance of tailoring training parameters and configurations to optimize performance outcomes (Figure 9). The high results achieved across the spectrum of models stand as a testament to the sophistication of the methodologies employed, as well as the careful consideration given to refining each model's architecture and training strategy.

After a comprehensive analysis of the YOLOv5, YOLOv7, and YOLOv8 object detection models, the YOLOv8 model emerges as the primary choice. Its well-balanced precision (88.2%) and recall (77.4%) contribute to an impressive F1-score (82%), indicating a strong trade-off between accurate detections and comprehensive coverage. The high mAP 50 (87.2%) showcases its reliability across varying IoU thresholds. YOLOv8 stands out with the swiftest detection time (0.052 seconds per image), making it both accurate and efficient. Considering its harmonious blend of performance metrics, YOLOv8 is recommended as the main selection for a wide array of object detection tasks.

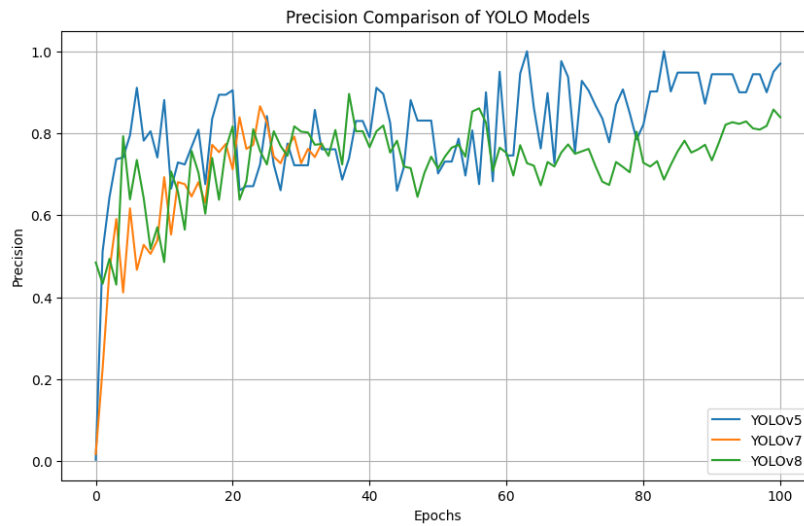


Figure 6. Models precision comparisons

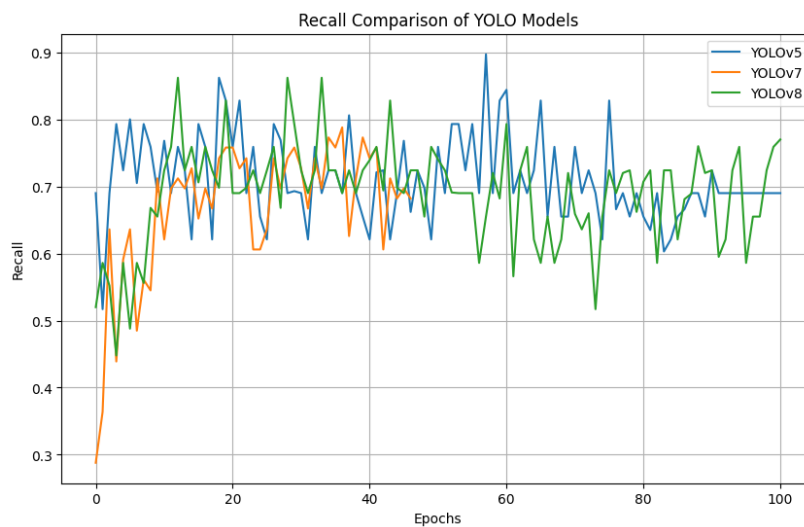


Figure 7. Models recall comparisons

The successful implementation of deep learning in this context represents a significant advance over traditional tree inspection methods. The speed and accuracy of the model allows for rapid assessment of forest health over a wide area, which is critical for timely intervention and conservation strategies. Figure 7 presents a graphical representation of the model data, illustrating that YOLOv5 exhibits notably high precision, while YOLOv7 displays performance indicators that are comparatively inferior to those of YOLOv8. Notably, YOLOv8 demonstrates a balanced and superior performance in relation to the other evaluated models.

Despite its success, several challenges remain in implementing deep learning for forest health monitoring. One of the key challenges lies in data collection and annotation. The curation of diverse, high-quality data sets is essential, along with accurate manual annotation, to improve model performance and generalization. Another challenge is the interpretation of the results. While the models show high accuracy, the 0.77 recall achieved by the YOLOv8 model suggests that it may have missed some dead and dying trees in the image. Improving recall without compromising accuracy is important for a more comprehensive understanding of forest health. The proposed algorithm for compressing images without loss of quality and

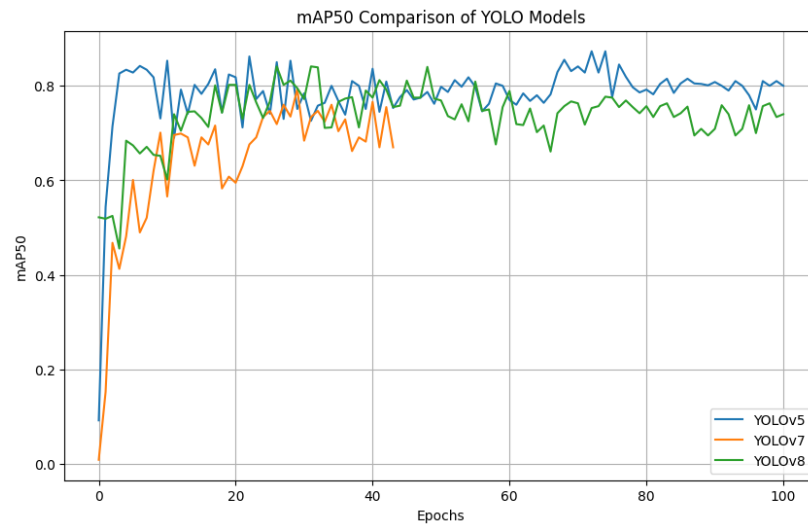


Figure 8. Models mAP50 comparisons

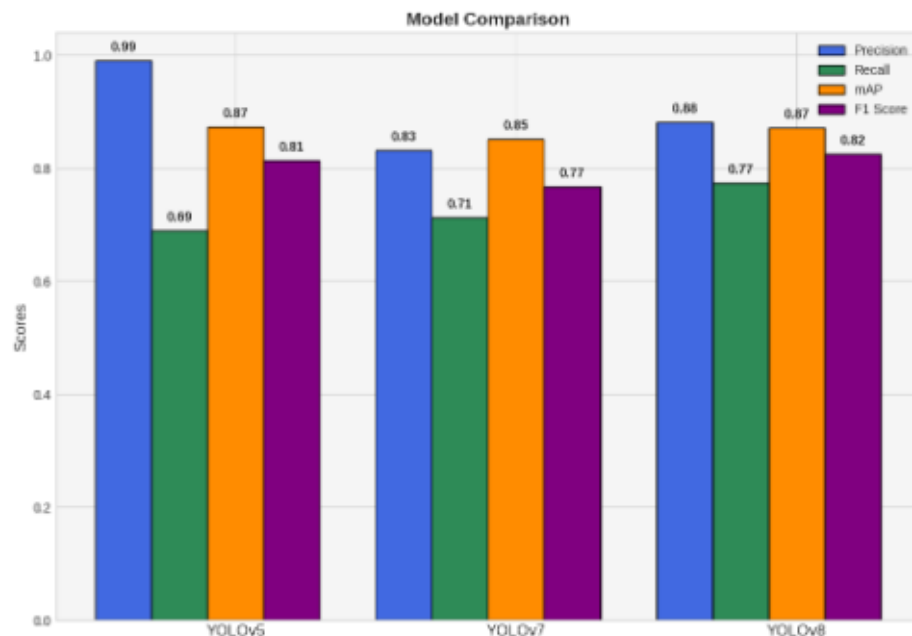


Figure 9. YOLOv5, YOLOv7, YOLOv8-based classification models metrics bar chart

its implementation data pre-processing stage significantly improves the classification results quality, but of course a longer period of images collection is necessary to increase the performance of the evaluation.

To further improve the accuracy and efficiency of deadwood classification, future research could focus on data augmentation techniques and new feature extraction methods. Augmenting datasets with more diverse environmental conditions, such as various weather and lighting conditions, can improve model reliability in real-world scenarios. Moreover, ensemble methods that combine multiple AI models would be explored to overcome the trade-off between accuracy and recall. Such an approach could lead to improved overall performance in identifying and locating deceased trees in aerial imagery.

In addition, continued efforts should be made to align the application of machine learning in forestry and environmental research with ethical considerations. Ensuring privacy, data security, and sustainable practices are essential to gain broad public acceptance and support for AI-based systems.

As contribution it was designed models based on new image compression algorithm and deep learning techniques for diseases trees detection in aerial imagery has shown substantial results in environmental monitoring and forest management. The high metrics obtained by the YOLOv8 model provide valuable insights for identifying and assessing dead trees in large areas. Challenges remain, but continued research and progress in data collection, model development, and ethical considerations will lead to further improvements and a positive impact on global environmental conservation efforts.

4 Conclusion

In presented paper were studied the qualitative indicators of the developed algorithm for compressing aerospace images without loss of quality for phytosanitary forest monitoring, which showed high performance data pre-processing for further classification based on AI. The experimental studies of the proposed based on difference-discrete transformation algorithm research results, concluded about reliability and high accuracy of developed mathematical apparatus. The integration of the proposed compression method to the image processing information model was successful, as a result, a high compression ratio of $R=8$ was achieved. The resulting images were used to train neural networks (YOLO v5, YOLO v7, YOLO v8) and outcome classification models received high indicators metrics of detection monitoring objects. As the end of result of performed study, there was conduct the comparative analysis of the results of the work of three classification models. The successful application of YOLOv8 in diseased trees classification presents an opportunity to revolutionize forest monitoring and conservation efforts. By accurately detecting and classifying infected trees, AI-powered systems can provide valuable insights into forest health, enabling timely interventions to protect and restore these vital ecosystems. However, challenges and opportunities for future development exist. Data collection, diversity, and ethical considerations are crucial factors to improve model performance and gain public acceptance. Ensuring comprehensive data sets with various environmental conditions and exploring ensemble methods could enhance the overall accuracy and recall of the models. As technology advances, AI-powered forest monitoring has the potential to play a significant role in mitigating the adverse effects of deforestation, forest fires, and diseases, contributing to a more sustainable and resilient environment for future generations. Embracing these innovative approaches, alongside responsible and informed decision-making, will be key to safeguarding the planet's green lungs and preserving the invaluable benefits that forests provide for humanity and the ecosystem.

Acknowledgement: The article was written within the state order for the implementation of the scientific program under the budget program of the Republic of Kazakhstan 217 "Development of Science", subprogram 101 "Program-targeted funding of the scientific and/or technical activity at the expense of the national budget" on the theme: " Development of technology for intelligent preprocessing of aerospace images for recognition and identification of various objects " Grant IRN AP19678773.

References

- [1] Zhang, Y., Zhang, X., Liu, Y., & Li, J. (2018). Hyperspectral image compression using deep learning. *IEEE Transactions on Geoscience and Remote Sensing*, 56(1), 261-272. (journal)
- [2] Wenbin Wu, Yue Wu1, and Jintao Li. The Hyper-spectral Image Compression Based on K-Means Clustering and Parallel Prediction Algorithm. 03071 MATEC Web of Conferences 173, (2018) <https://doi.org/10.1051/mateconf/2018173 SMIMA 2018>. (proceedings)
- [3] N. A. A. Samah1, N. R. M. Noor, E. A. Bakar and M. K. M. Desa. CCSDS-MHC on Raspberry Pi for Lossless Hyperspectral Image Compression. *IOP Conf. Series: Materials Science and Engineering* 943 (2020) 012004 IOP Publishing. (proceedings)
- [4] CCSDS. Report concerning spectral pre-processing transform for multispectral & hyperspectral image compression. 2019. USA. (standard)

- [5] M. I. Afjal, M. A. Mamun, and M. P. Uddin, "Band reordering heuristics for lossless satellite image compression with 3D-CALIC and CCSDS," *Journal of Visual Communication and Image Representation*, vol. 59, pp. 514–526, 2019/02/01/ 2019. (journal)
- [6] Zhang, Y., Zhang, J., & Li, X. (2023). Hyperspectral image compression using implicit neural representation. arXiv preprint arXiv:2302.04129. (arxiv)
- [7] Doulamis, N., Doulamis, A., & Venetsanopoulos, A. N. (2019). Lossless image compression for space applications. *IEEE Signal Processing Magazine*, 36(1), 128–141. (journal)
- [8] Wu, W., Wu, Y., & Qiao, X. (2018). A parallel lossless compression algorithm for hyperspectral images. *IEEE Access*, 6, 37387–37401. (journal)
- [9] Dian, R., Li, S., & Fang, L. (2019). Tensor-based sparse representation for hyperspectral image compression. *IEEE Transactions on Geoscience and Remote Sensing*, 57(11), 7033–7045. (journal)
- [10] Zhang, C., Fu, H., Hu, Q., & Xu, D. (2019). Adaptive spectral–spatial compression of hyperspectral image with sparse representation based on superpixels. *IEEE Transactions on Geoscience and Remote Sensing*, 57(10), 7103–7115. (journal)
- [11] Akbar, S. M., Khan, M. A., & Khan, A. A. (2019). SPIHT-based compression of hyperspectral images using a modified discrete wavelet transform. *Journal of Signal Processing Systems*, 90(2), 155–166. (journal)
- [12] Zhang, Y., Liu, Z., & Zhang, Y. (2019). An improved EZW algorithm for hyperspectral image compression. *Journal of Visual Communication and Image Representation*, 55, 102–111. <https://doi.org/10.1016/j.jvcir.2018.09.00313>. (journal)
- [13] H. Shen, W. D. Pan, and D. Wu, "Predictive lossless compression of regions of interest in hyperspectral images with no-data regions," *IEEE Trans. Geosci. Remote Sens.* 55, 173–182 (2017). (journal)
- [14] N. Kefalas and G. Theodoridis, "Low-memory and high-performance architectures for the CCSDS 122.0-B-1 compression standard," *Integration*, 2018/04/10/ 2018. (journal)
- [15] Hao Chen, Weidong Wang, and Lei Zhang (2019). A GPU-Accelerated Lossless Compression Framework for Earth Observation Imagery. 10.1109/TGRS.2019.2897725. (journal)
- [16] Detection and Classification of Aircraft Fixation Elements during Manufacturing Processes Using a Convolutional Neural Network Leandro Ruiz 1,2 , Manuel Torres 2, Alejandro Gómez 2, Sebastián Díaz 2, José M. González 2 and Francisco Cavas 3, *Appl. Sci.* 2020, 10, 6856; doi:10.3390/app10196856 www. (journal)
- [17] Wang, Z.; Zhou, Y.; Li, G. Anomaly detection for machinery by using Big Data Real-Time processing and clustering technique. In *Proceedings of the 2019 3rd International Conference; ACM International Conference Proceeding Series (ICPS): New York, NY, USA, 2019; pp. 30–36.* (proceedings)
- [18] Pouyanfar, S.; Sadiq, S.; Yan, Y.; Tian, H.; Tao, Y.; Reyes, M.P.; Shyu, M.L.; Chen, S.C.; Iyengar, S.S. A survey on deep learning: Algorithms, techniques, and applications. *Acm Comput. Surv.* 2018. (journal)
- [19] H. Du, W. Zhang, N. Guan, and W. Yi, "Scope-aware data cache analysis for OpenMP programs on multi-core processors," *Journal of Systems Architecture*, vol. 98, pp. 443–452, 2019/09/01/ 2019. (journal)
- [20] S. Balakrishnan, D. Langerman, E. Gretok, and D. A. D. George, "Deep Learning for Hyperspectral Image Classification on Embedded Platforms," in *2018 IEEE International Conference on Image Processing, Applications and Systems (IPAS)*, 2018, pp. 187–191. (proceedings)
- [21] Ball JE, Wei P. Deep Learning Hyperspectral Image Classification using Multiple Class-Based Denoising Autoencoders, Mixed Pixel Training Augmentation, and Morphological Operations. In: *IGARSS 2018-2018 IEEE International Geoscience and Remote Sensing Symposium*. IEEE; 2018. p. 6903–6906. (proceedings)
- [22] Belwalkar A, Nath A, Dikshit O. Spectral-spatial Classification Of Hyperspectral Remote Sensing Images Using Variational Autoencoder And Convolution Neural Network. *International Archives of the Photogrammetry, Remote Sensing & Spatial Information Sciences*. 2018. <https://doi.org/10.5194/isprsarchives-XLII-5-613-2018>. (journal)
- [23] Maggiori E, Plaza A, Tarabalka Y. Models for Hyperspectral Image Analysis: From Unmixing to Object-Based Classification. In: Moser G, Zerubia J, editors. *Mathematical Models for Remote Sensing Image Processing: Models and Methods for the Analysis of 2D Satellite and Aerial Images*. Cham: Springer International Publishing; 2018. p. 37–80. (chapter)
- [24] N. S. Abramov, D. A. Makarov, A. A. Talalaev, V. P. Fralenko. *Sovremennye metody intellektualnoi obrabotki danih DZZ. Programmiye sistemi, teoriya i prilozheniya.* – T. 9 439, S. – 417442.
- [25] Ghamisi P, Yokoya N, Li J, Liao W, Liu S, Plaza J, et al. Advances in Hyperspectral Image and Signal Processing: A Comprehensive Overview of the State of the Art. *IEEE Geoscience and Remote Sensing Magazine*. 2017; 5(4):37–78. <https://doi.org/10.1109/MGRS.2017.2762087>. (journal)
- [26] Lu B, Dao PD, Liu J, He Y, Shang J. Recent Advances of Hyperspectral Imaging Technology and Applications in Agriculture. *Remote Sensing*. 2020; 12(16):2659. <https://doi.org/10.3390/rs12162659>. (journal)
- [27] Drumetz L, Meyer TR, Chanussot J, Bertozzi AL, Jutten C. Hyperspectral image unmixing with endmember bundles and group sparsity inducing mixed norms. *IEEE Transactions on Image Processing*. 2019; 28(7):3435–3450. <https://doi.org/10.1109/TIP.2019.2897254> PMID: 30716036. (journal)
- [28] Zhang, Y., Zhang, L., Li, J., Chen, Z., & Liu, H. (2020). A review of preprocessing techniques for hyperspectral image analysis. *Remote Sensing*, 12(1), 110. <https://doi.org/10.3390/rs12010110>. (journal)

- [29] Signoroni A, Savardi M, Baronio A, Benini S. Deep learning meets hyperspectral image analysis: a multidisciplinary review. *Journal of Imaging*. 2019; 5(5):52. <https://doi.org/10.3390/jimaging5050052> PMID:34460490. (journal)
- [30] Licciardi G, Chanussot J. Spectral transformation based on nonlinear principal component analysis for dimensionality reduction of hyperspectral images. *European Journal of Remote Sensing*. 2018; 51(1):375–390. <https://doi.org/10.1080/22797254.2018.1441670>. (journal)
- [31] Aroma RJ, Raimond K. A Wavelet Transform Applied Spectral Index for Effective Water Body Extraction from Moderate-Resolution Satellite Images. In: *Artificial Intelligence Techniques for Satellite Image Analysis*. Springer; 2020. p. 255–274. (chapter)
- [32] Paoletti M, Haut J, Plaza J, Plaza A. Deep learning classifiers for hyperspectral imaging: A review. *ISPRS Journal of Photogrammetry and Remote Sensing*. 2019; 158:279–317. <https://doi.org/10.1016/j.isprsjprs.2019.09.006>. (journal)
- [33] Dao PD, Mantripragada K, He Y, Qureshi FZ. Improving hyperspectral image segmentation by applying inverse noise weighting and outlier removal for optimal scale selection. *ISPRS Journal of Photogrammetry and Remote Sensing*. 2021; 171:348–366. <https://doi.org/10.1016/j.isprsjprs.2020.11.013>. (journal)
- [34] Xianhao Zhu, Rui rui Wang, Wei Shi, Qing Yu, Xiang Li and Xing wang Chen(2023). Automatic Detection and Classification of Dead Nematode-Infected Pine Wood in Stages Based on YOLO v4 and GoogLe Net. DOI:10.3390/f14030601. (journal)
- [35] Marie-Claude Jutras-Perreault, Terje Gobakken, Erik Næsset and Hans Ole Ørka(2023). Comparison of Different Remotely Sensed Data Sources for Detection of Presence of Standing Dead Trees Using a Tree-Based Approach. DOI:10.3390/rs15092223. (journal)
- [36] A. Gupta, S. Watson, H. Yin, Deep learning-based aerial image segmentation with open data for disaster impact assessment, *Neurocomputing*. 439 (2021) 22–33, <https://doi.org/10.1016/j.neucom.2020.02.139>. (journal)
- [37] Patil, D., Jadhav, S. (2021). Road Extraction Techniques from Remote Sensing Images: A Review. In: Raj, J.S., Iliyasu, A.M., Best, R., Baig, Z.A. (eds) *Innovative Data Communication Technologies and Application. Lecture Notes on Data Engineering and Communications Technologies*, vol 59. Springer, Singapore. <https://doi.org/10.1007/978-981-15-9651-355>. (chapter)
- [38] F. Chen, R. Ren, T. Van de Voorde, W. Xu, G. Zhou, Y. Zhou, Fast automatic airport detection in remote sensing images using convolutional neural networks, *Remote Sens.* 10 (2018) 1–20, <https://doi.org/10.3390/rs10030443>. (journal)
- [39] A. Froidevaux, A. Julier, A. Lifschitz, M.T. Pham, R. Dambreville, S. Lefevre, P. Lassalle, T.L. Huynh, Vehicle Detection and Counting from VHR Satellite Images: Efforts and Open Issues, *IEEE Nternational Geosci. Remote Sens.Symp.* (2020) 256–259, <https://doi.org/10.1109/IGARSS39084.2020.9323827>. (proceedings)
- [40] Y. Wu, W. Ma, M. Gong, Z. Bai, W. Zhao, Q. Guo, X. Chen, Q. Miao, A coarse-to-fine network for ship detection in optical remote sensing images, *Remote Sens.* 12 (2020) 1–24, <https://doi.org/10.3390/rs12020246>. (journal)
- [41] G.S. Xia, X. Bai, J. Ding, Z. Zhu, S. Belongie, J. Luo, M. Datcu, M. Pelillo, L. Zhang, DOTA: A large-scale dataset for object detection in aerial images, in: *IEEE Comput. Soc. Conf. Comput. Vis. Pattern Recognit., IEEE*, 2018: pp. 3974–3983, <https://doi.org/10.1109/CVPR.2018.00418>. (proceedings)
- [42] Watanabe, S., Sumi, K., & Ise, T. (2020). Identifying the vegetation type in Google Earth images using a convolutional neural network: a case study for Japanese bamboo forests. *BMC Ecology*, 20(1). <https://doi.org/10.1186/s12898-020-00331-5>. (journal)
- [43] Li, W., Dong, R., Fu, H., & Yu, and L. (2018). Large-Scale Oil Palm Tree Detection from High-Resolution Satellite Images Using Two-Stage Convolutional Neural Networks. *Remote Sensing*, 11(1), 11. <https://doi.org/10.3390/rs11010011>. (journal)
- [44] Wang, P., Fan, E., & Wang, P. (2020). Comparative Analysis of Image Classification Algorithms Based on Traditional Machine Learning and Deep Learning. *Pattern Recognition Letters*. <https://doi.org/10.1016/j.patrec.2020.07.042>. (journal)
- [45] Akcay, S., Kundegorski, M. E., Willcocks, C. G., & Breckon, T. P. (2018). Using Deep Convolutional Neural Network Architectures for Object Classification and Detection Within X-Ray Baggage Security Imagery. *IEEE Transactions on Information Forensics and Security*, 13(9), 2203–2215. doi:10.1109/tifs.2018.2812196. (journal)
- [46] Kadhim, M.A., Abed, M.H. (2020). Convolutional Neural Network for Satellite Image Classification. In: Huk, M., Maleszka, M., Szczerbicki, E. (eds) *Intelligent Information and Database Systems: Recent Developments. ACIIDS 2019. Studies in Computational Intelligence*, vol 830. Springer, Cham. <https://doi.org/10.1007/978-3-030-14132-513>. (chapter)
- [47] Sinyavskiy, Y. N., Melnikov, P. V., & Pestunov, I. A. (2019). Extension of training set using mean shift procedure for aerospace images classification. *E3S Web of Conferences*, 75, 01010. doi:10.1051/e3sconf/20197501010. (proceedings)
- [48] Karypidis, E., Mouslech, S. G., Skoulariki, K., & Gazis, A. (2022). Comparison analysis of traditional machine learning and deep learning techniques for data and image classification. *arXiv preprint arXiv:2204.05983*. (arxiv)
- [49] Liu, N., Wang, L., Huang, Q., & Ji, Y. (2020). Multi-view Deep Representations with Cross-Dataset Transfer for Remote Sensing Image Retrieval and Classification. *Multimedia Tools and Applications*. doi:10.1007/s11042-020-08712-0. (journal)

- [50] Mohammad Sadegh Ebrahimi, Hossein Karkeh Abadi (2018). Study of Residual Networks for Image Recognition. <https://doi.org/10.48550/arXiv.1805.00325>. (arxiv)
- [51] Sharma, N., Jain, V., & Mishra, A. (2018). An Analysis Of Convolutional Neural Networks For Image Classification. *Procedia Computer Science*, 132, 377–384. doi:10.1016/j.procs.2018.05.198. (journal)
- [52] Zhang, Y., Li, Z., & Zhang, L. (2020). Aerial object detection with deep neural networks: A review. *Neurocomputing*, 396, 121–135. doi:10.1016/j.neucom.2020.01.097. (journal)
- [53] Sharada Prasanna Mohanty et al. (2020). Deep Learning for Understanding Satellite Imagery: An Experimental Survey. *Frontiers in Artificial Intelligence*, 3. <https://doi.org/10.3389/frai.2020.534696>. (journal)
- [54] Xiang, J. et al. (2023). Dynamic Detection of Forest Change in Hunan Province Based on Sentinel-2 Images and Deep Learning. *Remote Sensing*, 15(3), 628. <https://doi.org/10.3390/rs15030628>. (journal)
- [55] Zhang, J., Li, S., Zhang, X., Wang, Y., & Liu, Y. (2018). A comparison of machine learning methods for forest classification using multi-temporal Landsat data. *Remote Sensing*, 10(10), 1555. <https://doi.org/10.3390/rs10101555>. (journal)
- [56] Qin, B., Sun, F., Shen, W., Dong, B., Ma, S., Huo, X., & Lan, P. (2023). Deep Learning-Based Pine Nematode Trees' Identification Using Multispectral and Visible UAV Imagery. *Drones*, 7(3), 183. (journal)
- [57] L. Yan, M. Zhao, X. Wang, Y. Zhang and J. Chen, "Object Detection in Hyperspectral Images," in *IEEE Signal Processing Letters*, vol. 28, pp. 508-512, 2021, doi: 10.1109/LSP.2021.3059204. (journal)
- [58] Iordache, M. D., Mantas, V., Baltazar, E., Pauly, K., & Lewycky, N. (2020). A machine learning approach to detecting pine wilt disease using airborne spectral imagery. *Remote Sensing*, 12(14), 2280. (journal)
- [59] Sarinova, A., & Zamyatin, A. (2020). Hyperspectral regression lossless compression algorithm of aerospace images. In *E3S Web of Conferences* (Vol. 149, p. 02003). EDP Sciences.